Redox and Spectral Properties of Cytochrome b_{559} in Different Preparations of Photosystem II†

Olga Kaminskaya,*,‡ Jens Kurreck,§ Klaus-D. Irrgang,§ Gernot Renger,*,§ and Vladimir A. Shuvalov‡

Institute of Basic Biological Problems, Russian Academy of Sciences, Pushchino, Moscow Region 142292, Russia, and Max-Volmer-Institute for Biophysical Chemistry and Biochemistry, Technical University Berlin, Strasse des 17, Juni 135, D-10623 Berlin, Germany

Received June 2, 1999; Revised Manuscript Received September 8, 1999

ABSTRACT: A detailed analysis of the properties of cytochrome b_{559} (Cyt b_{559}) in photosystem II (PS II) preparations with different degrees of structural complexity is presented. It reveals that (i) D1−D2−Cyt b_{559} complexes either in solubilized form or incorporated into liposomes contain only one type of Cyt b_{559} with E_m values of 60 ± 5 and 100 ± 10 mV, respectively, at pH 6.8; (ii) in oxygen-evolving solubilized PS II core complexes Cyt b_{559} exists predominantly (>85%) as an LP form with an $E_{m,7}$ of 125 ± 10 mV and a minor fraction with an $E_{m,7}$ of −150 ± 15 mV; (iii) in oxygen-evolving PS II membrane fragments three different redox forms are discernible with E_m values of 390 ± 15 mV (HP form), 230 ± 20 mV (IP form), and 105 ± 25 mV (LP form) and relative amplitudes of 58, 24, and 18%, respectively, at pH 7.3; (iv) the E_m values are almost pH-independent between pH 6 and 9.5 in all sample types except D1−D2−Cyt b_{559} complexes incorporated into liposomes with a slope of −29 mV/pH unit, when the pH increases from 6 to 9.5 (IP and LP form in PS II membrane fragments possibly within a restricted range from pH 6.5 to 8); (v) at pH >8 the HP Cyt b_{559} progressively converts to the IP form with increasing pH; (vi) the reduced-minus-oxidized optical difference spectra of Cyt b_{559} are very similar in the λ range of 360−700 nm for all types except for the HP form which exhibits pronounced differences in the Soret band; and (vii) PS II membrane fragments and core complexes are inferred to contain about two Cyt b_{559} hemes per PS II. Possible implications of conformational changes near the heme group and spin state transitions of the iron are discussed.

The key steps of photosynthetic water cleavage take place in a membrane-bound multimeric complex termed photosystem II (PS II)[1] (for a recent review, see ref *1* and references therein). Cytochrome b_{559} (Cyt b_{559}) is an integral constituent of PS II. Rather harsh treatments are required to separate Cyt b_{559} from this complex (*2*, *3*). The tight connection with the D1−D2 protein matrix of the cofactors of PS II might be an indication of an essential role of Cyt b_{559}. However, despite numerous studies performed during the last two to three decades (see refs *4*−*7* for the reviews), the exact function(s) of this hemoprotein is still obscure. It was proposed that Cyt b_{559} mediates a cyclic electron flow within PS II (*4*, *8*−*10*) which could be relevant as a protective mechanism against photoinhibition (*11*, *12*). Alternatively, the possibility has been discussed that this heme protein could provide an intrinsic superoxide dismutase activity in PS II (*13*) or participate in the process of water cleavage (*4*, *14*−*17*).

Apart from this important unresolved problem, even the much more simple question about the number of Cyt b_{559} hemes per PS II (one or two) has not yet been answered and is a matter of controversial discussions. Most of the studies performed with intact chloroplasts and thylakoids report a ratio of two Cyt b_{559} hemes per PS II (*18*−*20*) (but see ref *21*). No agreement on the question of one or two Cyt b_{559} heme groups per PS II could be achieved for PS II membrane fragments (*22*−*32*), for PS II core complexes (*28*, *30*, *33*−*35*), or even for D1−D2−Cyt b_{559} preparations (*36*−*39*). An unambiguous answer could be given by structure analysis of sufficiently high resolution. Unfortunately, such data are not available so far (see the Discussion). It is therefore not surprising that in a recent book article written by experts (*6*) this stoichiometry is characterized as a "cloudy issue".

One reason for the "Cyt b_{559} enigma" is the properties of Cyt b_{559} which are unique among hemoproteins. The heme iron of isolated and purified Cyt b_{559} is axially coordinated

† The support by grants from DFG (438/113/138/O and Re 354/10-3), CRDF (RB1-281), and the Russian Fund of Basic Research (96-15-97923) is gratefully acknowledged. We are indebted to Dr. A. Shkuropatov for support of this work by a grant from the Russian Fund of Basic Research (97-04-49866).

* Corresponding authors. O.K.: fax, (7) (096) 7790532; e-mail, kamin@issp.serpukhov.su. G.R.: fax, 49 30 314 21122; e-mail, renger@pc-109ws.chem.tu-berlin.de.

‡ Russian Academy of Sciences.

§ Technical University Berlin.

[1] Abbreviations: PS II, photosystem II; Cyt, cytochrome; E_m, midpoint potential; E_h, ambient redox potential; HP, high potential; IP, intermediate potential; LP, low potential; XLP, extra low potential; β-DM, *n*-dodecyl β-D-maltoside; Chl, chlorophyll; MES, 2-(*N*-morpholino)ethanesulfonic acid; HEPES, *N*-(2-hydroxyethyl)piperazine-*N*′-2-ethanesulfonic acid; CHES, 2-(*N*-cyclohexylamino)ethanesulfonic acid; DDQ, 2,3-dichloro-5,6-dicyano-*p*-benzoquinone; EDTA, ethylenediaminetetraacetic acid; DGDG, digalactosyldiacylglycerol; fwhm, full width at half-maximum; FTIR, Fourier transform infrared; MGDG, monogalactosyldiacylglycerol; WOC, water-oxidizing complex.

10.1021/bi991257g CCC: $18.00
Published on Web 11/12/1999

by two imidazole nitrogens and attains the low-spin state (*40*). As two polypeptides called α- and *β*-subunits exist, each containing only one His residue and forming one transmembrane helix, the heme could be bound either by a homodimeric matrix (of the type αα or *ββ*) or by an α*β* heterodimer. Both alternatives are discussed in the literature, reflecting discrepancies in experimental data (*41*−*43*; for review see refs *6* and *7*). The carboxyl terminus of the α-subunit is located at the lumen side (*44*), while the orientation of the *β*-subunit is less clear (see refs *6* and *42* for detailed citation). The orientation of the α-subunit and the position of its His residue relative to the membrane vertical axis imply the location of at least one heme group near the stroma side about 8 Å from the end of the α-helix (*45*).

The most interesting feature of Cyt b_{559} is the remarkable variability of the midpoint potential of the heme group. This property is used as a criterion for assignment of Cyt b_{559} to different forms. Cyt b_{559} isolated from spinach thylakoids or PS II membrane fragments exhibits midpoint potentials of 115 and 158 mV, respectively, at pH 7.5 (*46*).

In marked contrast, Cyt b_{559} in PS II complexes surrounded by their natural membrane environments exists in different forms with midpoint potentials of about 400 mV (designated as the HP form), 200 ± 50 mV (IP form), and 60 ± 50 mV (LP form) measured in chloroplasts, thylakoids (*12*, *47*−*52*), and PS II membrane fragments (*29*, *53*−*55*) at pH 6−6.5.

An E_m value on the order of 400 mV is unique for *b*-type cytochromes. The normalized extent of this HP form varies between 50 and 90% and generally decreases under stress conditions such as elevated temperature, detergent and salt treatment, low pH, and aging of the samples (*4*, *50*−*53*, *56*−*58*). This finding might suggest that the HP form is the physiologically relevant Cyt b_{559} and that the IP and LP forms are the result of structural rearrangements near the heme group(s) (*51*, *55*, *57*). The possible physiological role of the HP form remains an unresolved problem. Regardless of this problem, it is clear that HP Cyt b_{559} is not required for a functionally competent water-oxidizing complex (WOC) because PS II preparations without this form are still active in oxygen evolution (*28*, *33*, *35*, *59*−*62*). This finding confirms former conclusions (*63*). Surprisingly, detailed redox titrations are lacking for PS II core complexes which are the oxygen-evolving preparations with the smallest subunit composition. Conflicting results were reported for both the existence of different forms and their E_m values of Cyt b_{559} in D1−D2−Cyt b_{559} complexes (*36*, *64*, *65*).

A new phenomenon was discovered recently. It was found that in Tris-washed PS II membrane fragments, deprived of their oxygen evolution capacity, a reversible transition between HP and IP (LP) forms of Cyt b_{559} takes place when samples are switched from anaerobic to aerobic and/or reducing/oxidizing conditions. This effect was not observed in PS II membrane fragments with an intact WOC, and it might therefore be relevant in a protective role of photoinhibition and/or regulation of the WOC assembly in PS II (*66*, *67*).

The nature of structural determinants of the midpoint potential in Cyt b_{559} and the mechanism of interconversion between the different redox forms are not yet resolved. Several factors which affect the redox potential of the heme group in Cyt b_{559} have been considered, such as the electrical field generated by parallel transmembrane α-helices, the dihedral angle between the axial histidine heme ligands, and the protonation or deprotonation of amino residues which are coupled with the heme (*8*, *40*, *53*, *68*) (see ref *7* for a detailed review). The latter might be important under in vivo conditions, because different pH dependencies for the midpoint potentials of the various redox forms were reported for chloroplasts (*47*, *51*), thylakoids (*12*, *52*), and PS II membrane fragments (*53*). Unfortunately, the data obtained so far did not lead to a consistent picture.

The unique coordination of the heme group in Cyt b_{559} is most likely responsible for its peculiar redox properties which includes the unusually high redox potential compared with those of other *b*-type cytochromes and the interconversion between different redox forms. The heme iron in Cyt b_{559} is usually thought to attain the low-spin state. This conclusion is based on the typical low-spin EPR signal near $g = 3$ of the oxidized Cyt b_{559} and the characteristic narrow α-band with a maximum at 559 nm of the reduced heme. However, recent studies using PS II samples with different structural hierarchies revealed, along with the low spin, also high-spin features associated with Cyt b_{559}. High-spin EPR signals at $g = 5.9$ and 6.8 originating from Cyt b_{559} were reported in fresh chloroplasts and PS II membrane fragments oxidized by DDQ and in oxygen-evolving PS II core complexes as well as in D1−D2−Cyt b_{559} complexes at high pH (*14*−*17*, *69*).

The above description reveals that despite numerous reports about the properties of Cyt b_{559} a detailed analysis of the midpoint potentials of Cyt b_{559} and their pH dependence in D1−D2−Cyt b_{559} complexes either solubilized or incorporated into liposomes, O_2-evolving PS II core complexes, and PS II membrane fragments is still missing. The study presented here is an attempt to fill this gap and, in addition, to present the reduced-minus-oxidized difference spectra reported for these sample types in the whole visible region. Furthermore, on the basis of a large data set, the question of the Cyt b_{559}:PS II stoichiometry will be addressed. The implications of the results that were obtained are discussed.

MATERIALS AND METHODS

D1−D2−Cyt b_{559} complexes were isolated from sugar beet according to the original method of Nanba and Satoh (*70*) with some modifications (*36*). Triton X-100 was used for membrane solubilization. Solubilized D1−D2−Cyt b_{559} complexes were then purified by ion-exchange chromatography with Fractogel TSK DEAE-650(S) (Merck, Darmstadt, Germany). Isolated D1−D2−Cyt b_{559} complexes were obtained and stored in elution buffer containing 50 mM Tris (pH 7.2), 130 mM NaCl, and 0.1% (w/v) *n*-dodecyl *β*-D-maltoside (*β*-DM) (Sigma).

Lipid vesicles were prepared according to ref *71*. Azolectine (20 mg/mL) from soybean [Sigma, type IV-S, 40% (w/w) phosphatidylcholine content] was dissolved by sonication in 50 mM potassium phosphate buffer (pH 7.5) containing 0.8% (w/v) *n*-octyl *β*-D-glucopyranoside (Sigma) and then dialyzed against the same buffer without detergent. Incorporation of the isolated D1−D2−Cyt b_{559} complexes into the preformed vesicles was achieved by mixing of a

small volume of D1−D2−Cyt b_{559} complexes concentrated to 80−100 μM with liposome suspensions [standard lipid-to-protein ratio of 45 (w/w)] and incubation of the mixture for 30 min at 0 °C in the presence of 0.5 mM dithiothreitol. The proteoliposome suspension was then diluted by the medium used for redox titrations. An increase in the lipid-to-protein ratio to 90 (w/w) or 120 (w/w) did not affect the experimental results.

Redox titration and spectral measurements with D1−D2−Cyt b_{559} complexes either solubilized or incorporated in proteoliposomes were performed at 11 °C in 150 mM buffer (MES, HEPES, Tris, or CHES, depending on the pH range) containing 0.1% (w/v) β-DM in the case of solubilized complexes. The optical density at 675 nm was 0.8−1 cm^{-1}.

PS II membrane fragments were obtained from spinach and sugar beet according to the method of Berthold et al. (*72*) with some modifications (*61*). Isolated PS II membrane fragments were stored at 77 K in a buffer containing 20 mM MES (pH 6.5), 0.4 M sucrose, 15 mM NaCl, 4 mM $MgCl_2$, 1 mM sodium ascorbate, and 20% (v/v) glycerol. Redox titration experiments and spectral measurements were carried out at 16 °C mostly on the PS II membrane fragments isolated from sugar beet in a medium containing 0.3 M sucrose, 100 mM buffer (MES, HEPES, Tricine, or CHES, depending on the pH range), 10 mM $CaCl_2$, 10 mM NaCl, and 10% (v/v) glycerol. The chlorophyll concentration was 130−150 μg/mL.

Oxygen-evolving PS II core complexes were obtained from spinach PS II membrane fragments by a modified method described previously (*62*, *73*) in the presence of β-DM and further centrifugation on sucrose gradients. Samples were stored at 77 K in a buffer containing 25 mM MES (pH 6.5), 35% (w/v) sucrose, 10 mM $CaCl_2$, and 0.025% (w/v) β-DM. These PS II core complexes are mainly monomeric and deprived of the extrinsic 23 and 17 kDa proteins (*62*, *73*). Potentiometric titration of Cyt b_{559} and spectral measurements on PS II core complexes were performed at 16 °C in an assay medium containing 100 mM buffer (MES, HEPES, Tricine, or CHES, depending on the pH), 10 mM $CaCl_2$, 10 mM NaCl, 0.025% (w/v) β-DM, and 10% (v/v) glycerol. The chlorophyll concentration was about 20 μg/mL.

PS II membrane fragments and PS II core complexes exhibited typical average O_2 evolution rates under saturating cw light of around 650 and 1100 μmol of O_2 (mg of Chl)$^{-1}$ h^{-1}, respectively, at 20 °C with 0.5 mM 2,6-dichloro-1,4-benzoquinone and 1 mM $K_3[Fe(CN)_6]$ as acceptors. The buffer medium used for measuring oxygen evolution rates contained 100 mM MES-NaOH (pH 6.5), 0.3 M sucrose, and 10 mM $CaCl_2$ or 100 mM MES-NaOH (pH 6.5), 20 mM $CaCl_2$, and 10 mM NaCl for PS II membrane fragments or PS II core complexes, respectively.

Redox titration was performed in an anaerobic cuvette (1 cm optical path length) with a Hitachi-557 spectrophotometer (Japan) supplemented with a home-built stirrer. The optical spectra were recorded between 530 and 580 nm. The chemical difference spectra were obtained by subtracting spectra of the oxidized state or reduced state from those recorded at various ambient redox potentials. The amplitude of the absorbance changes at 559−560 nm in the redox difference spectrum was determined relative to a straight line connecting the points at 544 and 573 nm. Those points are close to the isosbestic points of the Cyt b_{559} chemical difference spectrum (*74*) and were chosen to minimize the baseline distortion from the C550 signal at the blue end of the optical interval. The slit widths were 2, 3, and 4 nm in the titration experiments with D1−D2−Cyt b_{559} complexes, PS II core complexes, and PS II membrane fragments, respectively.

The heme concentration was determined spectrophotometrically using an extinction coefficient of 17.5 mM^{-1} cm^{-1} at 560 nm in the "reduced-minus-oxidized" difference spectrum of the isolated Cyt b_{559} (*4*, *74*). The Chl:PS II ratio of PS II membrane fragments and PS II core complexes was calculated from measurements of the Chl content according to the method described in ref *75* and either the average oxygen yield per flash as outlined in ref *76* or the initial amplitude of flash-induced absorption changes as described in ref *77*. In the former case, the values that were obtained were 220 ± 30 and 65 ± 10 for PS II membrane fragments and PS II core complexes, respectively. The corresponding values gathered from absorption changes are 200 ± 20 and 45 ± 10. These values closely resemble data reported in the literature (*22*, *24*, *73*).

Anaerobic potentiometric titration was carried out essentially as described by Dutton (*78*). The following mediators were used in the redox potential region from 450 to −100 mV: 2,3-dichloro-5,6-dicyano-1,4-benzoquinone, 1,4-benzoquinone, 2,3,5,6-tetramethyl-*p*-phenylenediamine, 2,5-dimethyl-1,4-benzoquinone, the $FeSO_4$−EDTA complex, and 4,5-dihydroxy-1,3-benzenedisulfonic acid at concentrations of 50−100 μM; 2-hydroxy-1,4-naphthoquinone and 2-methyl-1,4-naphthoquinone at concentrations of 20 μM; and *N*-methylphenazonium methosulfate and 1,2-naphthoquinone at concentrations of 10 μM. For the redox titrations in the low-potential region, the following mediators were used: 20 μM 2-hydroxy-1,4-naphthoquinone, 50 μM sodium anthraquinone-2-sulfonate, 10 μM 2-amino-3-chloronaphthoquinone, and 3 μM benzyl viologen. The initial concentrations of dithionite or $K_3[Fe(CN)_6]$ were in the range of 0.5−1 mM in oxidative or reductive titrations, respectively. Anaerobic conditions were established by a constant flow of oxygen-free argon through the cuvette above the sample solution as well as by adding 0.1 mg/mL glucose oxidase (Sigma), 0.1 mg/mL catalase (Sigma), and 5 mM glucose to the reaction buffer.

The ambient redox potential was measured with a platinum electrode using a calomel electrode as reference which was connected to the Radelkis PH OP-211/1 pH/mV-meter. The electrode was calibrated at 20 °C in a standard $K_4[Fe(CN)_6]$/$K_3[Fe(CN)_6]$ solution (E_m = 420 mV) before each titration and checked again at the end of the experiment. The deviation in the redox potential value of the calibration solution before and after titrations typically did not exceed 3 mV. $K_3[Fe(CN)_6]$ and freshly prepared sodium dithionite were used as titrants in oxidative and reductive titrations, respectively. Each titration took 1.5−2 h. If not noted otherwise, the oxidative and reductive titrations were carried out in different samples. The pH of the sample was measured each time at the end of the titration with the same pH/mV-meter using an E5634 combinated electrode (Sigma).

Potentiometric Nernst curves were analyzed by a nonlinear curve-fitting Origin program. Typical errors in the fitting of redox titration curves were about ±10 mV for E_m and about

±5% for the normalized amplitudes of the different components.

Reduced-minus-oxidized difference spectra of Cyt b_{559} in the wide optical range were recorded at room temperature in a Cary 5 spectrophotometer with an optical slit width of 3.5 nm. To eliminate absorbance contributions associated with $K_3[Fe(CN)_6]$ and $K_4[Fe(CN)_6]$ in the Cyt b_{559} difference spectra shown in panels C and D of Figure 5, the absorbance spectra of added substances were monitored in separate measurements and subtracted from the obtained difference spectra of Cyt b_{559}.

RESULTS

For a characterization of Cyt b_{559} in PS II complexes surrounded by different environments, the following properties were analyzed in D1−D2−Cyt b_{559} complexes and oxygen-evolving PS II core complexes and PS II membrane fragments: (i) redox titration curves, (ii) pH dependence of midpoint potentials and relative levels of different Cyt b_{559} forms, and (iii) reduced-minus-oxidized difference spectra in the whole visible region.

Redox Titration Curves. To account for possible effects due to baseline distortions by addition of exogenous redox compounds, in all cases the full α-band region of Cyt b_{559} was monitored (see Materials and Methods). It was checked that the typical features (peak position at 559−560 nm and fwhm of about 11 nm) were not disturbed. Furthermore, the redox titrations were performed in both the oxidative and reductive direction. Figure 1A presents typical results obtained for isolated D1−D2−Cyt b_{559} complexes of sugar beet at pH 6.8. The sample solubilized in 0.1% (w/v) *β*-DM exhibits a titration curve (curve 1) with a single wave in the wide range of redox potentials from 500 to −300 mV. Virtually the same data points are obtained in the oxidative and reductive directions of titration. The results can be perfectly described by the Nernst equation for a single electron redox step, i.e., $n = 1$, with a midpoint potential of 60 mV. This value is very close to that of 70 mV measured earlier in D1−D2−Cyt b_{559} complexes from spinach in the presence of 0.05% (v/v) Triton X-100 (*36*). However, it differs from later findings in samples solubilized in 0.1% (w/v) *β*-DM (*64*, *65*) where a redox heterogeneity of Cyt b_{559} was observed with the main component exhibiting E_m values of 150−180 mV (for further details, see the Discussion).

To unravel possible effects of the environment on the midpoint potential of the heme group, redox titrations were performed with D1−D2−Cyt b_{559} complexes incorporated into liposomes. In these samples, the α-band of the reduced heme of Cyt b_{559} exhibits the same peak wavelength of 559 nm and fwhm of about 11 nm as observed in the solubilized samples (data not shown). Titration curve 2 of Figure 1A reveals that incorporation of D1−D2−Cyt b_{559} complexes into lipid vesicles causes a single E_m shift to 102 mV at pH 6.8, i.e., by about 40 mV toward more positive values without any indication of multicomponent redox behavior of Cyt b_{559} in the range from 500 to − 300 mV. This finding is interesting because it reflects a modification of the Cyt b_{559} protein environment which is homogeneous in terms of effects on the redox properties.

Typical redox titration curves of oxygen-evolving PS II core complexes from spinach at pH 7.8 are depicted in Figure 1B. The data readily reveal the existence of two clearly distinguishable waves, which can be described by the Nernst equation with E_m values of 118 and −147 mV and relative amplitudes of 86 and 14%, respectively, and $n = 1$ for both components. No differences are observed for oxidative and reductive titration. Both redox forms exhibit a very similar α-band in the reduced-minus-oxidized difference spectrum (data not shown). The midpoint potential of the predominant form is close to that of Cyt b_{559} in D1−D2−Cyt b_{559} complexes incorporated into liposomes at pH 6.8. The minor form is characterized by the E_m value which is far below that of D1−D2−Cyt b_{559} solubilized in the same detergent

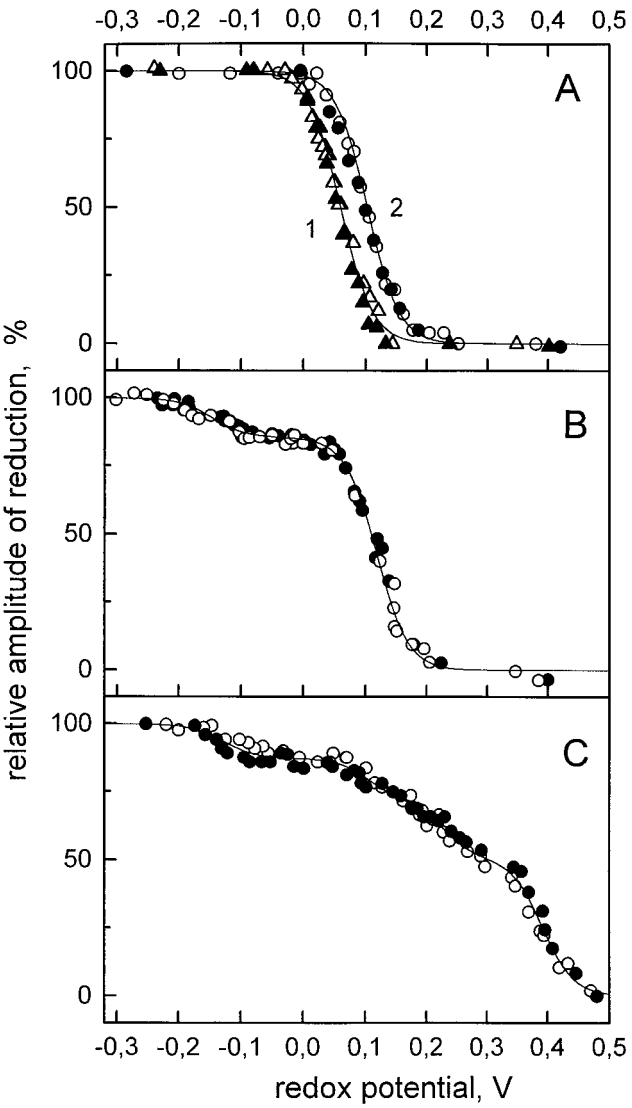

FIGURE 1: Relative amplitude of reduced Cyt b_{559} as a function of redox potential in suspensions of D1−D2−Cyt b_{559} complexes in solubilized form (triangles) or incorporated into liposomes (circles) (A), PS II core complexes (B), and PS II membrane fragments (C). White and black symbols represent data points of the titration in the oxidative and reductive direction, respectively. The curves are best fits by the Nernst equation for single-electron redox steps and one component with E_m values of 60 mV (triangles) or 102 mV (circles) (A), two components with E_m values of 118 mV (86%) and −147 mV (14%) (B), and four components with E_m values of 392 mV (51%), 229 mV (21%), 105 mV (16%), and −128 mV (12%) (C). For experimental details, see Materials and Methods. The data points represent the results of single-titration experiments. The scatter in total amplitude of the absorbance change in the α-band upon redox state transition was within 15% in all types of samples.

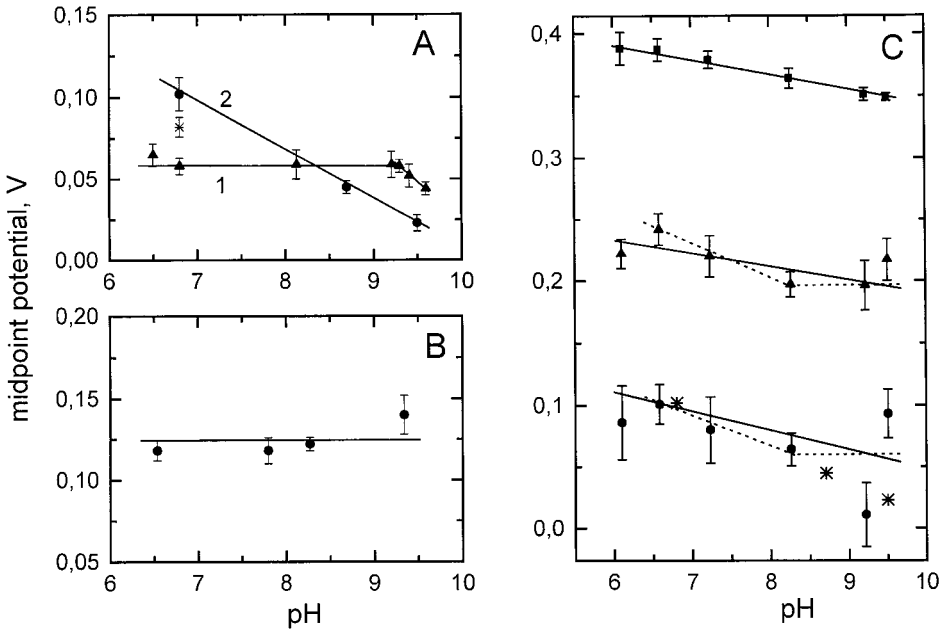

FIGURE 2: Midpoint potentials of Cyt b_{559} as a function of pH in D1−D2−Cyt b_{559} complexes in solubilized form (triangles) or incorporated into liposomes (circles) (A), PS II core complexes (B), and PS II membrane fragments (C; squares, triangles, and circles symbolize the E_m values of the HP, IP, and LP forms, respectively). The star point in panel A is the result of measurements in samples that were preincubated for 2 h at pH 9.5 (25 mM CHES) and then rebuffered to pH 6.8. The star points in panel C are the data for D1−D2−Cyt b_{559} proteoliposomes taken from panel A. The midpoint potentials were gathered from Nernst fits of titration curves as outlined in Figure 1. For experimental details, see Materials and Methods.

β-DM and will be called the XLP (extra low potential) form.

Figure 1C shows the corresponding titration curves of the α-band of Cyt b_{559} in PS II membrane fragments from sugar beet at pH 7.3. An inspection of the data readily reveals that the pattern is more complex than in D1−D2−Cyt b_{559} complexes (Figure 1A) and PS II core complexes (Figure 1B). The results can be well described by the Nernst equation for four clearly discernible single-electron redox transitions. The redox step with the lowest E_m value (below −100 mV) is characterized by a peak at 563 nm in the α-band (not shown) and originates from small amounts of Cyt b_6 that are present in the sample. Therefore, in the following, this feature will be omitted for the sake of clarity. A numerical fit results in E_m values for Cyt b_{559} of 392 mV (HP form), 229 mV (IP form), and 105 mV (LP form) and relative amplitudes of 58, 23, and 19%, respectively. These values are in excellent agreement with previous reports on the redox properties of Cyt b_{559} in PS II membrane fragments from different plant material (*29*, *54*).

pH Dependence of Midpoint Potential. To check for a possible modification of the redox properties of Cyt b_{559} by protonation of the protein matrix, titration experiments of the α-band were performed in the pH range from 6 to 9.5. It has been carefully checked whether differences arise between the results of oxidative and reductive titration. No significant hysteresis effect was observed; small differences were always within the limit of data scattering of repeated experiments in only one titration direction (only oxidative or reductive).

Figure 2 depicts the average E_m values of Cyt b_{559} in different types of PS II preparations as a function of pH. An inspection of these data shows that the E_m of Cyt b_{559} in solubilized D1−D2−Cyt b_{559} complexes is independent of pH in the range from 6.5 to 9. Above this pH, a decrease is observed (see curve 1 of Figure 2A). In marked contrast, the midpoint potential of D1−D2−Cyt b_{559} complexes incorporated into liposomes exhibits a distinct pH dependence with a slope of −29 mV/pH unit in the whole pH region from 6.5 to 9.5 (see curve 2 of Figure 2A). This effect of pH is largely reversible as shown by the star point.

It is interesting to note that the incorporation of D1−D2−Cyt b_{559} complexes into liposomes not only markedly alters the pH dependence of the midpoint potential of Cyt b_{559} but also greatly enhances its stability for long-term incubation. After incubation of the samples for 20 h at pH 6.7 and 4 °C, the E_m value of the solubilized complexes drops by 30 mV, while that of the proteoliposomes remains constant within experimental error (data not shown).

Another important result is the finding that Cyt b_{559} exhibits a homogeneous behavior in the whole pH range in both sample types of D1−D2−Cyt b_{559} complexes. In this respect, the situation is markedly different in oxygen-evolving PS II core complexes and PS II membrane fragments. In both cases, more than one form of Cyt b_{559} is discernible on the basis of the E_m values (see panels B and C of Figure 1). Therefore, a variation of pH can affect the E_m values and the normalized amplitudes of the different forms. In this section, only the former parameter will be described. The results obtained for PS II core complexes are shown in Figure 2B. It reveals that the E_m of the dominating LP form of Cyt b_{559} is virtually independent of pH between 6.5 and 8.3. A very small shift toward a more positive value at pH 9.3 is considered insignificant. The pH dependence of the minor XLP form was not analyzed in detail, because the normalized amplitude remains small over the whole pH range (vide supra). There was no indication for a pronounced effect of pH on the E_m value (data not shown).

In PS II membrane fragments with an intact WOC, the HP form of Cyt b_{559} is dominating at neutral pH (see Figure 1C). Figure 3 shows redox titration curves monitored at pH

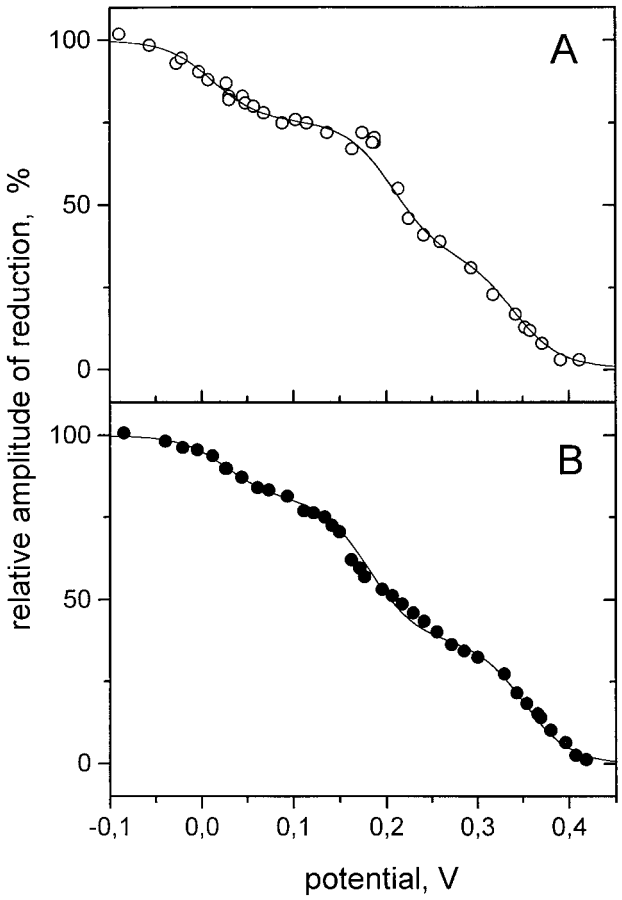

FIGURE 3: Relative amplitude of reduced Cyt b_{559} as a function of redox potential in suspensions of PS II membrane fragments at pH 9.2 measured in the oxidative (A) or reductive (B) direction. The curves are best fits by Nernst equation for single-electron redox transitions and three Cyt b_{559} forms with E_m values of 340 mV (35%), 207 mV (41%), and 12 mV (24%) in panel A and 350 mV (38%), 181 mV (43%), and 27 mV (19%) in panel B. The data points represent the results of single-titration experiments. The total amplitude of the absorbance change difference in the α-band upon redox transition was within 15% when comparing different measurements.

9.2 in both the oxidative (panel A) and reductive (panel B) directions. Apart from the absence of a significant hysteresis effect at pH 9.2, two striking features emerge from these data and a comparison with Figure 1C: (i) the E_m values differ only slightly between pH 7.3 and 9.2, and (ii) the normalized extent of the IP form markedly increases at the expense of the HP form. Here, only the first phenomenon will be analyzed in more detail; the second effect is dealt with in the subsequent section.

Figure 2C summarizes the pH dependence of E_m values for the HP, IP, and LP form of Cyt b_{559} in PS II membrane fragments. At first glance, all three forms can be described by straight lines that exhibit a rather weak pH dependence of about −10 mV/pH unit. This conclusion is straightforward for the HP form and consistent with previous findings in chloroplasts and PS II membrane fragments from spinach (*51*−*53*). A closer inspection, however, reveals that a more complex situation could arise for the IP and LP forms as indicated by dotted lines. In this case, a pH dependence with −29 mV/pH unit would arise for the E_m of the IP and LP forms in the range from pH 6.5 to 8.2 and constant values of 200 ± 20 and 60 ± 20 mV, respectively, above pH 8.2.

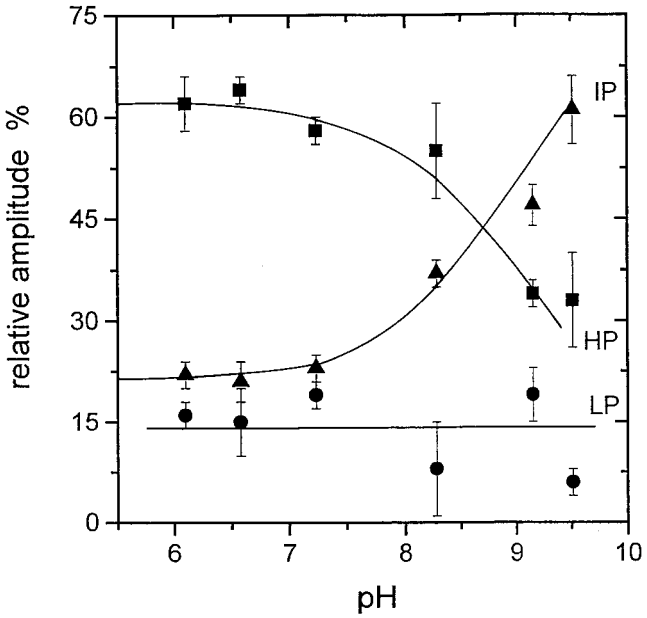

FIGURE 4: Relative amplitudes of HP (squares), IP (triangles), and LP (circles) Cyt b_{559} as a function of pH in suspensions of PS II membrane fragments. The data were gathered by best fits with the Nernst equation of titration curves as described in the legend of Figure 1C. Six to eight titration curves were measured for each pH value, except pH 9.5 where the data represent the average of two experiments.

This feature basically corresponds to a previous report (*53*), but marked quantitative differences exist, e.g., for the steepness of the slope. It must be emphasized that in the former study the midpoint potentials of Cyt b_{559} were determined by redox titrations performed only in the reductive direction, and also the *n* values of 0.7−0.8 for a fit with the Nernst equation are not easily understood. Unfortunately, the scatter of the data in Figure 2C does not permit unambiguous conclusions with respect to the pH dependence of the midpoint potentials of the IP and LP forms. A strong pH effect, with slopes of no less −60 mV/pH unit as reported in ref *53*, however, can be ruled out on the basis of the results obtained in the study presented here.

pH-Dependent Interconversion of Cyt b_{559} with Different Midpoint Potentials. The results of Figure 2 have shown that the midpoint potential of the Cyt b_{559} forms in PS II preparations with different degrees of structural complexity and environments is at most only slightly dependent on pH. Another interesting question is the possibility of a pH-dependent conversion between different forms in PS II core complexes and PS II membrane fragments that contain two and three, respectively, populations of Cyt b_{559} which are distinguished by distinctly different midpoint potentials. An analysis of the titration curve reveals that the ratio of LP to XLP Cyt b_{559} in PS II core complexes is virtually independent of pH within the range of 6.5−9.5 (data not shown), but in this sample type, the LP form was found to be unstable at alkaline pH (*69*).

A markedly different pattern is observed in PS II membrane fragments. Figure 4 shows the normalized populations of the HP, IP, and LP forms as a function of pH. The most prominent feature is the steep decline in the population of the HP form at pH >8 and the concomitant mirror image increase in that of the IP form. On the other hand, the level of the LP form remains constant within the limits of data

Table 1: Midpoint Potentials and Relative Amplitudes of Cyt b_{559} in Control and Pretreated PS II Membrane Fragments

pH of titration	treatment before titration	LP[a]	IP[a]	HP[a]
6.5	none	101 ± 16 mV	242 ± 13 mV	387 ± 9 mV
		15 ± 5%	21 ± 3%	64 ± 2%
9.2	none	11 ± 26 mV	196 ± 20 mV	351 ± 5 mV
		19 ± 5%	47 ± 7%	34 ± 2%
6.5[b]	pH 9.1	98 ± 24 mV	237 ± 22 mV	390 ± 5 mV
	dithionite[c]	18 ± 9%	22 ± 6%	60 ± 2%
6.5[b]	pH 9.1	115 ± 28 mV	227 ± 24 mV	389 ± 12 mV
	$K_3[Fe(CN)_6]$[c]	23 ± 12%	47 ± 16%	30 ± 1%

[a] The values of midpoint potentials and amplitudes represent the average of three or four experiments. [b] The titrations were performed only in the oxidative direction. [c] Before titration at pH 6.5, the samples were preincubated aerobically for 30 min at 16 °C in the medium used for redox titrations, except for the presence of 25 mM CHES (pH 9.1), with the addition of 3 mM dithionite and 0.1 mg/mL catalase or 0.5 mM $K_3[Fe(CN)_6]$. After incubation, the pH of the samples was shifted back to 6.5 by addition of 200 mM MES (pH 6.4).

scattering. These findings show that in PS II membrane fragments the Cyt b_{559} undergoes a HP → IP form transition at alkaline pH.

The amplitudes of the Cyt b_{559} redox forms at each pH depicted in Figure 4 are average values gathered from titration curves in the oxidative and reductive direction. Although a small hysteresis in the relative amplitudes was observed between reductive and oxidative titration, the shift is within the error limit of the experimental data. We could not confirm previously published data (*55*) on a drastic decline of the HP form from 90% in the first oxidative down to 50% in the subsequent reductive titration of the same sample at pH 6.0. In the investigations described here, the contribution of the HP form was, on average, 10−15% lower and that of the IP and LP forms correspondingly higher in reductive titrations than in oxidative titrations, the effect being more pronounced at the high pH. This observation, which may be an indication of different susceptibilities of oxidized and reduced Cyt b_{559} to alkaline pH, raises the question of the reversibility of the pH-induced conversion of the HP to the IP form in the alkaline region.

To analyze this possibility in more detail, comparative titration experiments were performed at pH 6.5 with untreated control and samples preincubated for 30 min at pH 9.1 and 16 °C in the presence of either 3 mM dithionite or 0.5 mM $K_3[Fe(CN)_6]$ before returning to pH 6.5 by addition of MES buffer. The results are summarized in Table 1.

An inspection of these data reveals that the alkaline-induced HP → IP transformation is largely irreversible when Cyt b_{559} remains oxidized during preincubation at pH 9.1. In contrast, when Cyt b_{559} is kept reduced at pH 9.1 by the presence of $Na_2S_2O_4$, the redox behavior at pH 6.5 remains virtually unaffected by alkaline pH preincubation.

The conversion of HP Cyt b_{559} to its IP form induced by high pH (Figure 4) can be explained by a conformational change in the hemoprotein due to deprotonation of amino acid residue(s) near the heme group. This effect could comprise possible changes in the coordination sphere of the heme iron. To address this point, every effort was made to measure reduced-minus-oxidized difference spectra in the whole visible region.

Reduced-Minus-Oxidized Difference Spectra of Cyt b_{559} of D1−D2−Cyt b_{559} Complexes, PS II Core Complexes, and PS II Membrane Fragments in the Visible Region. The reduced-minus-oxidized difference spectrum of Cyt b_{559} in the whole visible region has been measured for isolated Cyt b_{559} (*2*, *4*) and D1−D2−Cyt b_{559} complexes (*70*, *79*). It is more difficult to monitor the corresponding spectra of the individual Cyt b_{559} forms (HP, LP, IP, and XLP) in PS II membrane preparations. In this case, the desired spectra have to be extracted from a much higher background because of Chl and Car absorption, especially in the blue region. Furthermore, interference in the Cyt b_{559} Soret band occurs with the absorption of redox dyes that are used for a suitable redox poise which is necessary for separating the different Cyt b_{559} forms. It is therefore not surprising that, to the best of our knowledge, there exists no report on difference spectra in the Soret band region of the HP, IP, and LP forms of Cyt b_{559} in oxygen-evolving PS II membrane fragments. To circumvent the above-mentioned difficulties, the following approaches were used. The HP Cyt b_{559} was oxidized by the presence of 0.2 mM $K_3[Fe(CN)_6]$. Subsequent addition of 4 mM $K_4[Fe(CN)_6]$ led to an ambient redox potential of about 350 mV and, therefore, to reduction of a major fraction of the HP form (more than 65% as determined from the amplitude of the α-band). The absorption changes caused by $K_4[Fe(CN)_6]$ were recorded in a separate measurement of the difference spectrum of buffer solutions containing 0.2 mM $K_3[Fe(CN)_6]$ in the absence or presence of 4 mM $K_4[Fe(CN)_6]$. This spectrum was used for corrections.

To monitor the difference spectrum of the IP form, we took advantage of the irreversible pH-induced HP → IP form transition (see Table 1). Samples were preincubated for 30 min at pH 9.1 in the presence of 0.5 mM $K_3[Fe(CN)_6]$ and then returned to pH 6.5 by addition of MES buffer (the $K_3[Fe(CN)_6]$ concentration was lowered to 0.2 mM). Addition of 4 mM $K_4[Fe(CN)_6]$ caused the reduction of most of the HP Cyt b_{559} but kept the IP (and LP) form oxidized (state 1). The IP form was then reduced by 10 mM ascorbate (state 2). An evaluation of the amplitudes of the α-band revealed that the difference between states 1 and 2 largely reflects the redox transition of IP Cyt b_{559}. Therefore, after correction for the addition of ascorbate, the resulting difference spectrum reflects mainly Cyt b_{559} in the IP form.

The reduced-minus-oxidized difference spectra of LP Cyt b_{559} in D1−D2−Cyt b_{559} complexes, of the dominating LP form in PS II core complexes, and of the HP and IP forms in PS II membrane fragments are compiled in Figure 5. An inspection of these results readily shows that except for the HP form, the difference spectra of the other Cyt b_{559} forms are very similar and virtually independent of the sample type. The small differences in the range from 430 to 500 nm between spectrum C and spectra A and B are due to the much higher Chl and Car content of PS II membrane fragments. Therefore, the contribution of these pigments is less perfectly eliminated in trace C than in traces A and B, but the typical spectral features of Cyt b_{559} are not affected. They are characterized by a bleaching in the Soret band, peaking at about 412 nm, and maxima at 429 ± 2, 530 ± 1, and 559 ± 1 nm. These features are virtually identical to those of difference spectra of purified isolated Cyt b_{559} (*2*, *4*) and indicative of a low-spin axial bis-histidine coordination of the heme iron (*40*).

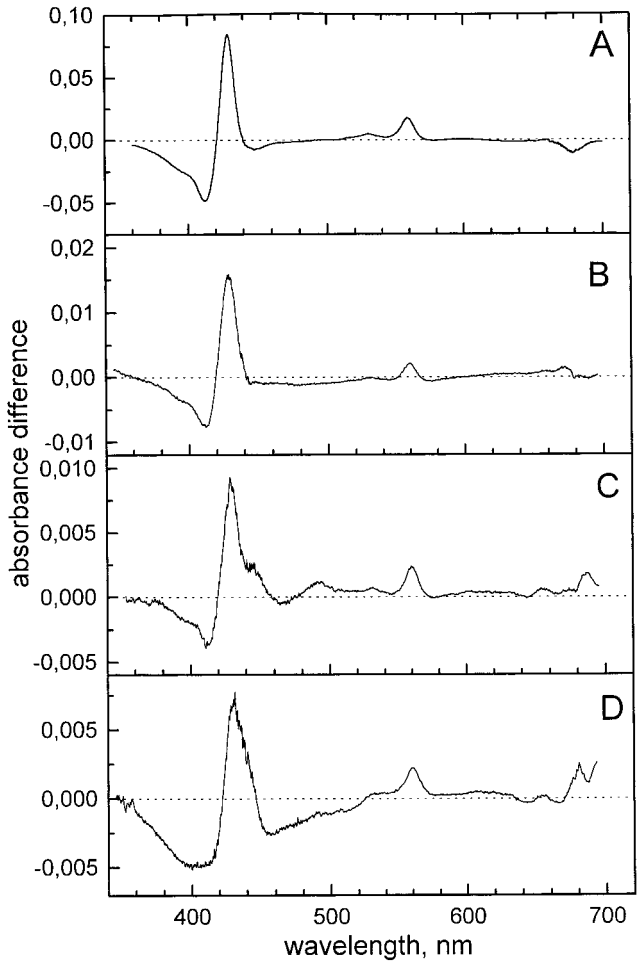

FIGURE 5: Reduced-minus-oxidized difference spectra of Cyt b_{559} in solubilized D1−D2−Cyt b_{559} preparations (A), PS II core complexes (B), the IP form (C), and the HP form (D) in PS II membrane fragments. Spectra A and B were measured at pH 8.4 (A) and 6.5 (B) after addition of 10 mM sodium ascorbate. The optical density at 675 nm was 0.53 cm^{-1} in panel A, and the chlorophyll concentration was 16 μg/mL in panel B. Spectra C and D were measured at pH 6.5 and a chlorophyll concentration of 24 μg/mL. Reduction of total Cyt b_{559} in the sample corresponds to a ΔA of 4×10^{-3} at 560 nm. For panel C, the difference spectrum of the IP Cyt b_{559} was measured upon addition of 10 mM ascorbate to the sample containing 200 μM ferricyanide and 4 mM ferrocyanide. To increase the amount of IP Cyt b_{559} in PS II membrane fragments, the sample was preincubated at pH 9.1 (see Table 1). For panel D, the difference spectrum of the HP Cyt b_{559} was recorded after addition of 4 mM ferrocyanide to native PS II membranes containing 200 μM ferricyanide.

Marked differences, however, are observed for the HP form. The characteristic features of the reduced form, i.e., the positive bands at 430, 530, and 560 nm, are very similar to those of IP and LP Cyt b_{559}, while the negative band, characteristic of the oxidized HP Cyt b_{559}, exhibits strikingly different features. The negative band is rather broad, and the maximum is shifted to near 403 nm. Furthermore, the negative tail at the long-wavelength side of the Soret band extends to about 500 nm. These spectral differences most likely reflect a change of the axial heme iron coordination upon oxidation of HP Cyt b_{559} which gives rise to a transition into the high-spin state of Fe(III).

Stoichiometry of Cyt b_{559} in PS II Preparations with Different Degrees of Structural Complexity. The study presented here not only provides new and detailed information about the redox and spectral properties of Cyt b_{559} in PS II surrounded by a different environment but also offers the possibility of discussing the problem of Cyt b_{559}:PS II stoichiometry on the basis of a large set of data. The quality of the results obtained depends on precise determination of the following parameters: (i) the extent of absorption change at 560 nm associated with the redox transition in Cyt b_{559}, (ii) the difference extinction coefficient at 560 nm, and (iii) the average number of chlorophyll molecules per PS II.

In PS II membrane fragments, the amplitude of the α-band of reduced Cyt b_{559} was nearly independent of pH. A small difference was observed in the amplitude at 560 nm in oxidized and reduced titrations with a slightly higher value in the latter case. The spectrum of the irreversible difference between oxidative and reductive titrations is characterized by a broad feature in the range of 560−580 nm (data not shown; see ref *80*) which arises from baseline distortion at redox potentials below 50 mV as also reported in previous studies (*22*, *29*, *80*). This effect does not exceed 15% of the total amplitude at 560 nm. Using the average value of ΔA_{560} and a difference extinction coefficient of 17.5 mM^{-1} cm^{-1} for Cyt b_{559} at 560 nm (*4*, *74*), a value of one Cyt b_{559} per 120 ± 20 Chl molecules is obtained (average of 30 measurements). The values of 220 ± 30 and 200 ± 20 reported in Materials and Methods reflect the average number of Chl molecules per PS II complex which are able to evolve oxygen and perform a stable charge separation, respectively. On the basis of a number of 200 ± 20 Chl molecules per PS II for PS II membrane fragments, a value of 1.7 ± 0.4 Cyt b_{559} hemes per PS II emerges from these data. This stoichiometry corroborates earlier estimations for PS II membrane fragments gathered from optical (*24*, *27*−*30*), EPR (*26*), and recent Mössbauer spectroscopy studies (*31*, *32*, *81*) where 1.6 ± 0.1 heme irons per non-heme iron center were found.

When using the same procedure and a ratio of 45 ± 10 Chl molecules per PS II (see Materials and Methods and ref *73*), similar values of 1.6 ± 0.4 total Cyt b_{559} hemes per PS II were obtained for O_2-evolving PS II core complexes (average of eight measurements). Thorough analyses were performed on a large number of PS II core complexes and led to similar values (K.-D. Irrgang and G. Renger, unpublished results).

A more complex and interesting pattern emerges for D1−D2−Cyt b_{559} preparations. The Cyt b_{559}:PS II stoichiometry in D1−D2−Cyt b_{559} preparations was determined by using the method outlined in ref *36*. On the basis of the idea that PS II contains two pheophytins, its content was determined from the absorption at 541 nm in samples without addition of exogenous redox active compounds and using the extinction coefficients reported in ref *82*. The amount of Cyt b_{559} was gathered from the α-band of the reduced-minus-oxidized difference spectrum. Two interesting results were found. (i) The Cyt b_{559}:PS II ratio is calculated to be 2.4 ± 0.5 for D1−D2−Cyt b_{559} preparations that were purified by using Fractogel TSK DEAE-650(S) regardless of the sample state (solubilized or incorporated into liposomes) (average value of 14 measurements), and (ii) a drastically smaller value of close to 1 emerges for D1−D2−Cyt b_{559} preparations purified by Q-Sepharose fast flow at pH 6.5. The latter 1:1 stoichiometry is in agreement with a number of recent reports (*38*, *39*, *83*, *84*). The difference between both types of D1−

D2−Cyt b_{559} preparations can only be explained by theassumption that part of Cyt b_{559} is labile and lost during the Q-Sepharose purification. This phenomenon could originate from either a removal of the heme group only or a depletion of the whole protein. Our preliminary investigations are highly in favor of the latter effect (K.-D. Irrgang et al., unpublished results).

DISCUSSION

The study presented here provides detailed comparative measurements of the properties of Cyt b_{559} in PS II preparations with different degrees of structural complexity and environments. Three important parameters were investigated in D1−D2−Cyt b_{559} preparations (solubilized form or incorporated in liposomes), O_2-evolving PS II core complexes, and PS II membrane fragments: (1) the midpoint potential(s) and its pH dependency, (2) the stoichiometric Cyt b_{559}:PS II ratio, and (3) the spin state of the heme iron at room temperature in the different redox states.

(1) Redox Properties

The results obtained by carefully performed redox titrations provide information about (a) the redox form(s) of Cyt b_{559} in PS II preparations with different degrees of complexity, (b) the pH dependence of the E_m values, and (c) the effect of lipids.

(a) Redox Forms in PS II Preparations. (i) PS II Membrane Fragments. In PS II membrane fragments, three redox forms of Cyt b_{559} are discernible. The E_m values of 388, 222, and 86 mV measured at pH 6.1 in samples from sugar beet (this study) are in excellent agreement with the values of 375, 228, and 57 mV, respectively, reported in ref *29* for the same type of preparation isolated from spinach. Likewise, the normalized amplitudes of 65, 19, and 15%, found at pH 6.1, are identical (within experimental error) to values of 66, 19, and 14% from ref *54* for HP, IP, and LP forms, respectively, in spinach samples. This strikingly close correspondence of data gathered from different sample materials seems to represent a general property of Cyt b_{559} in oxygen-evolving PS II membrane fragments from higher plants. It shows that at physiological pH values about two-thirds of the total Cyt b_{559} are in the HP form.

(ii) D1−D2−Cyt b_{559} Complexes. Compared with this almost perfect correspondence of results obtained by different groups for the complex system of PS II membrane fragments, it seems to be rather surprising that conflicting data are reported for the "simpler" D1−D2−Cyt b_{559} complexes. The most striking difference is the presence of only one redox form of Cyt b_{559} in D1−D2−Cyt b_{559} complexes from sugar beet either solubilized or in proteoliposomes found in this study, which is in marked contrast to previous reports of a heterogeneity of the redox properties of Cyt b_{559} in the corresponding sample type from spinach (*36*, *64*, *65*). At present, a straightforward explanation cannot be offered, but on the basis of the effects of lipids on the E_m value illustrated in Figure 1A, it appears to be reasonable to assume that the variation of the midpoint potentials of LP Cyt b_{559} may originate from a heterogeneity of the residual lipid content and its interaction with the protein in different D1−D2−Cyt b_{559} complexes. A more serious difference, however, is the finding of an appreciable amount (about 30%) of HP Cyt b_{559} in D1−D2−Cyt b_{559} preparations reported in ref *64*. The latter result is difficult to understand, because even for the much more intact PS II core complexes no indication of the existence of this form has been obtained. An inspection of the experimental conditions reveals that the redox titration of ref *64* was performed by monitoring only a single wavelength (559 nm). Therefore, distortions of the baseline by addition of exogenous redox-active compounds cannot be excluded. On the basis of these considerations, the existence of the HP form in D1−D2−Cyt b_{559} complexes appears to be questionable.

(iii) PS II Core Complexes. An unexpected feature was observed for spinach O_2-evolving PS II core complexes. In these samples, neither HP nor IP forms are detected; the Cyt b_{559} attains predominantly the LP form (>80% of the total content) (Figure 1B) with a pH-independent E_m of about 120 mV (Figure 2B). These PS II core complexes are deprived of the extrinsic 17 kDa (PsbQ) and 23 kDa proteins (PsbP) and of the vast majority of lipids (*73*, *85*). They exist to a large extent as monomers (*62*, *73*), each containing about 50 molecules of bound β-DM (*73*). When the redox properties of Cyt b_{559} in this sample type are considered, two parameters are of interest: the E_m value and its pH independence. The latter effect can be explained by the drastically reduced lipid content (vide infra). A more complicated problem is the lack of any HP and/or IP Cyt b_{559}. The E_m of Cyt b_{559} depends on different parameters (see ref *7* for a review), and therefore, the transformation into the LP form is most likely a combined effect caused by the loss of the 17 and 23 kDa proteins (*80*) and the drastic reduction of the lipid content (*73*, *85*). An essential determinant of the midpoint potential of cytochromes in general is the encapsulation of the heme group into the protein as illustrated by several studies (see ref *86* and references therein). In this respect, it is attractive to speculate about a possible role of a dimerization of PS II in the redox properties of Cyt b_{559}. It has been assumed by several groups that in thylakoid membranes the PS II complexes mainly exist as dimers (*87*−*89*). This might lead to a more pronounced shielding of the heme group as a prerequisite for attaining the HP and/or IP form(s). Accordingly, the dissociation into PS II monomers could be coupled with a marked decrease in E_m. This phenomenon would provide an explanation for the redox properties of our monomeric oxygen-evolving PS II core complexes. The possible relation between the redox properties of Cyt b_{559} and the aggregation state of PS II is a very interesting problem which remains to be elucidated in further studies.

(b) pH Effects. Two interesting features were observed for pH-induced changes of the redox properties of Cyt b_{559}. At first, Cyt b_{559} in the LP form exhibited significant changes of E_m only in a lipid environment either artificially restored by incorporation of D1−D2−Cyt b_{559} complexes into liposomes or supplied by the thylakoid membrane of PS II membrane fragments. A striking similarity emerges from a direct comparison of the data as illustrated in Figure 2C (bottom trace). Deviations might arise in the alkaline region where the E_m of LP Cyt b_{559} in PS II membrane fragments seems to remain constant while that of the D1−D2−Cyt b_{559} proteoliposomes continues to decrease with a slope of −29 mV per unit of increasing pH. The former effect is in line with a p*K* value near 8 as reported for thylakoids (*52*), but

the steepness of the slope is less pronounced than in previous studies (*47*, *52*). The results presented here suggest that the effect of pH on the E_m value of Cyt b_{559} in the LP (IP) form is not a property of the protein matrix alone but arises only in a lipid environment. Furthermore, the slope of the pH dependence suggests that several amino acid residues with different redox-dependent p*K* values are involved in a Bohr-type effect. The details, especially the possible role of hydrogen bonds, remain to be clarified. In contrast to that of the LP (IP) form, the midpoint potential of HP Cyt b_{559} is almost unaffected by pH in the range from 6 to 9.5.

The second striking phenomenon is the alkaline-induced HP → IP form conversion in PS II membrane fragments (see Figure 4). This state transition, which is coupled with a large decline in the E_m value of about 150 mV, can be almost fully reversed after returning to lower pH, when the heme group stays reduced at alkaline pH, but it becomes irreversible for the oxidized state. In previous studies, a similar dependence on the redox state of the heme group has been observed for the stability of the HP form of Cyt b_{559} (*53*, *58*). This phenomenon probably originates from different axial ligations of Fe in the oxidized and reduced forms of HP Cyt b_{559} (vide infra). It is being suggested that state transitions between HP and IP (LP) Cyt b_{559} might be involved in protective mechanisms of photoinhibition (*79*, *90*). However, at present it seems premature to speculate about this topic until more detailed information becomes available.

(c) Effect of Lipids. Previous studies led to the conclusion that incorporation of purified Cyt b_{559} into liposomes made of phosphatidylcholine/digalactosyldiacylglycerol and phosphatidylcholine/phosphatidylethanolamine gives rise to partial restoration of the HP form (*46*, *91*). Although our results confirm that at neutral pH the midpoint potential of Cyt b_{559} in D1−D2−Cyt b_{559} complexes in proteoliposomes is higher than that of the solubilized sample (see Figure 1A), we never observed any restoration of the HP form in D1−D2−Cyt b_{559} proteoliposomes. At first glance, these conflicting results might be ascribed to the use of different lipid mixtures, e.g., the lack of DGDG in asolectin. Although the enhancement of the level of hydroquinone reducible Cyt b_{559} depends on the nature of the lipids (*91*), the question of whether the HP form has been really restored remains open, because the E_m value was not determined in the former studies (*46*, *91*). It has to be emphasized that an unambiguous conclusion can only be drawn when reversible redox titrations (oxidative and reductive direction) are performed on the basis of measurements of the whole α-band. Most results reported in the literature do not satisfy this prerequisite. This could explain a number of puzzling results.

(2) Stoichiometric Cyt b_{559}:PS II Ratio and Structural Considerations

The study presented here provides a large set of data which permits us to address the controversy regarding the stoichiometric ratio of Cyt b_{559} to PS II. Using a difference extinction coefficient of 17.5 mM^{-1} cm^{-1} for the α-band of Cyt b_{559} (*4*, *74*) and the values for the average number of chlorophylls per PS II determined for PS II membrane fragments and PS II core complexes from higher plants, all data consistently indicate that the overall stoichiometry is significantly higher than one Cyt b_{559} per PS II. It has to be emphasized that the calculation is based on the total number of PS II complexes, including those that are inactive in oxygen evolution. Furthermore, detailed investigations reveal that part of Cyt b_{559} is lost when D1−D2−Cyt b_{559} complexes are prepared (K.-D. Irrgang et al., unpublished results). Accordingly, it seems possible that also other PS II preparations can be deprived of variable fractions of Cyt b_{559}, and this would give rise to conflicting results. In fact, the Cyt b_{559}:PS II ratio was 1.16 ± 0.10 in a report claiming a 1:1 stoichiometry for PS II core complexes from *Synechocystis* PCC 6803 (*92*), whereas another study on basically the same sample type led to values of 1.5−2.1 (*35*). The conclusion that about two hemes of Cyt b_{559} are associated with PS II is strongly supported by a recent study by Mizusawa et al. (*93*).

An unambiguous answer not only for the Cyt b_{559}:PSII stoichiometry but also for the question of a homodimeric (α_2,β_2) or heterodimeric ($\alpha\beta$) protein matrix will certainly be obtained when structural data of sufficient resolution are available. Recently, a three-dimensional map with a resolution of 8−9 Å was gathered from electron crystallography of CP47−D1−D2−Cyt b_{559} complexes (*94*). This result together with cryoelectron microscopy data (*95*) led to a model of the position of the membrane-spanning helices of inner core PS II polypeptides (*96*) in which the authors assigned only one Cyt b_{559} per PS II. However, a closer inspection reveals the existence of two pairs of unidentified membrane-spanning helices that are symmetrically located at the periphery of the D1−D2 heterodimer (*94*, *96*). These pairs of unidentified α-helices (depicted in blue in Figure 1 of ref *94* and in gray in Figure 4d of ref *96*) could be potential candidates for two cytochromes (J. Barber, personal communication). Therefore, the currently available structural information is not in contradiction with our conclusion of two Cyt b_{559} hemes per PS II.

(3) Spin State(s) of the Cyt b_{559} Heme Iron

It is currently a widely accepted view that Fe(III) in HP Cyt b_{559} attains the low-spin state. This conclusion is based on EPR signals at $g = 3.01-3.08$, observed in chloroplasts and PS II membrane fragments, which are ascribed to the HP form of Cyt b_{559} (*29*, *97*−*100*). Surprisingly, this assignment has never been checked by detailed redox titrations of the EPR signals. Apart from this, in thylakoid or crude PS II preparations also ferriheme-associated high-spin features near $g = 6$ have been reported by several groups (*97*−*99*, *101*). These signals with sometimes significant magnitudes were assumed to originate from heme moieties of degraded Cyt b_6 and/or Cyt *f*. However, recent studies demonstrated that EPR signals at $g = 5.9$ and 6.8 are due to Fe(III) of Cyt b_{559} (*14*−*17*). Furthermore, in freshly prepared chloroplasts with 90% of the total Cyt b_{559} in the HP form, only the high-spin EPR signals of the ferriheme were observed (*15*). The $g = 6.8$ signal has been suggested to reflect coordination of heme Fe(III) with an OH^- ligand that might be involved in water oxidation (*15*−*17*).

The EPR measurements were performed at low temperatures. Therefore, a general problem with any mechanistic consideration is the unresolved question as to what extent results gathered from samples in a liquid helium bath reflect the properties of the system under conditions where the

process of water oxidation really takes place (*102*). With respect to the spin state of Fe(III) in HP Cyt b_{559}, the possibility of temperature-dependent spin state transition has to be considered. Therefore, it is very important to search for a method that provides direct information about the spin state of oxidized Cyt b_{559} at physiological temperatures.

The study presented here offers an approach to answering this relevant question by measuring the reduced-minus-oxidized difference spectrum in the whole visible region. The traces depicted in panels A and B of Figure 5 for D1−D2−Cyt b_{559} complexes and PS II core complexes exhibit the typical Soret band feature of low-spin Cyt b_{559}. A similar spectrum is observed for IP Cyt b_{559} in PS II membrane fragments (Figure 5C). In marked contrast, a pronounced blue shift and broadening of the Soret band emerges for oxidized HP Cyt b_{559} as reflected by the negative band peaking at around 403 nm (Figure 5D). This feature is ascribed to a change in the mode of axial coordination and a transition into the high-spin ($S = {}^5/_2$) state. The peak of the Soret band near 403 nm of the oxidized Cyt b_{559} could be indicative of five-coordinate heme iron. On the other hand, a broad γ-band in the spectrum might suggest a mixture of five- and six-coordinate species (a detailed analysis of the spectrum of oxidized HP Cyt b_{559} will be presented in a forthcoming paper).

The results presented here clearly show that oxidized Cyt b_{559} in the HP form exists in the high-spin $S = {}^5/_2$ state at room temperature and undergoes a change in the mode of heme coordination and spin state of the iron upon reduction. The finding that the redox titration in Cyt b_{559} is coupled with structural changes was deduced earlier from a comparison of light and chemically induced low-spin EPR signals of Cyt b_{559} (*29*, *98*, *99*) and also from FTIR measurements (*103*). These occur in both HP and IP (LP) forms but are different in the two cases. The structural rearrangements in HP Cyt b_{559} are probably responsible for the high-pH susceptibility of oxidized HP Cyt b_{559} (see Figure 4).

The redox-linked spin state transition of HP Cyt b_{559} is a striking feature which remains to be analyzed in terms of its possible functional relevance. This phenomenon might be responsible for the unusually high redox potential of HP Cyt b_{559}. It has been proposed that the spin state of Cyt b_{559} might be related to water oxidation (*15*−*17*). However, as we have shown in this paper, in PS II core complexes with high oxygen evolution capacity the dominating LP Cyt b_{559} is low-spin in both, reduced and oxidized, states. On the other hand, it was found that the XLP form undergoes a low-spin → high-spin transition upon oxidation (*69*) that is similar to the one described in the study presented here. Therefore, the ability of Cyt b_{559} to undergo a redox-linked change of spin state in oxygen-evolving PS II preparations is not restricted to the HP form. The unraveling of a possible role of the new spin state phenomena in Cyt b_{559} remains a stimulating challenge for future studies.

ACKNOWLEDGMENT

We thank T. Volshchukova for the help in isolation of D1−D2−Cyt b_{559} complexes and T. Dolgova for the help in some titration experiments. We acknowledge Dr. R. Khatypov for his kind assistance in computer software.

REFERENCES

1. Renger, G. (1999) Molecular mechanism of water oxidation, in *Concepts in Photobiology: Photosynthesis and Photomorphogenesis* (Singhal, G. S., Renger, G., Govindjee, Irrgang, K.-D., and Sopory, S. K., Eds.) pp 292−329, Kluwer Academic Publishers, Dordrecht, The Netherlands, and Narosa Publishing Co., Delhi, India.
2. Garewall, H. S., and Wassermann, A. R. (1974) *Biochemistry 13*, 4063−4071.
3. Widger, W. R., Cramer, W. A., Hermodson, M., Meyer, D., and Gullifor, M. (1984) *J. Biol. Chem. 259*, 3870−3876.
4. Cramer, W. A., and Whitmarsh, J. (1977) *Annu. Rev. Plant Physiol. 28*, 133−172.
5. Shuvalov, V. A. (1994) *J. Bioenerg. Biomembr. 26*, 619−626.
6. Whitmarsh, J., and Pakrasi, H. B. (1996) in *Oxygenic Photosynthesis: The Light Reactions* (Ort, D. R., and Yocum, C. F., Eds.) pp 249−264, Kluwer Academic Publishers, Dordrecht, The Netherlands.
7. Stewart, D. H., and Brudvig, G. W. (1998) *Biochim. Biophys. Acta 1367*, 63−87.
8. Butler, W. L. (1978) *FEBS Lett. 95*, 19−25.
9. Arnon, D. I., and Tang, G. M.-S. (1988) *Proc. Natl. Acad. Sci. U.S.A. 85*, 9524−9528.
10. Canaani, O., and Havaux, M. (1990) *Proc. Natl. Acad. Sci. U.S.A. 87*, 9295−9299.
11. Thompson, L. K., and Brudvig, G. W. (1988) *Biochemistry 27*, 6653−6658.
12. Poulson, M., Samson, G., and Whitmarsh, J. (1995) *Biochemistry 34*, 10932−10938.
13. Ananyev, G., Renger, G., Wacker, U., and Klimov, V. V. (1994) *Photosynth. Res. 41*, 327−338.
14. Shuvalov, V. A., Fiege, R., Schreiber, U., Lendzian, F., and Lubitz, W. (1995) *Biochim. Biophys. Acta 1228*, 175−180.
15. Fiege, R., Schreiber, U., Renger, G., Lubitz, W., and Shuvalov, V. A. (1995) *FEBS Lett. 377*, 325−329.
16. Fiege, R., and Shuvalov, V. A. (1996) *FEBS Lett. 387*, 33−35.
17. Hulsebosch, R. J., Hoff, A. J., and Shuvalov, V. A. (1996) *Biochim. Biophys. Acta 1277*, 103−106.
18. Erixon, K., and Butler, W. L. (1971) *Biochim. Biophys. Acta 234*, 381−389.
19. Epel, B. L., Butler, W. L., and Levince, R. P. (1972) *Biochim. Biophys. Acta 275*, 395−400.
20. Whitmarsh, J., and Cramer, W. A. (1978) *Biochim. Biophys. Acta 501*, 83−93.
21. Heimann, S., Klughammer, C., and Scheiber, U. (1998) in *Photosynthesis: Mechanisms and Effects* (Garab, G., Ed.) Vol. II, pp 1089−1092, Kluwer Academic Publishers, Dordrecht, The Netherlands.
22. Buser, C. A., Diner, B. A., and Brudvig, G. W. (1992) *Biochemistry 31*, 11441−11448.
23. Bricker, T. M., Metz, J. G., Miles, D., and Sherman, L. A. (1983) *Biochim. Biophys. Acta 724*, 447−455.
24. Lam, E., Baltimore, B., Ortiz, W., Chollar, S., Melis, A., and Malkin, R. (1983) *Biochim. Biophys. Acta 724*, 201−211.
25. Ghanotakis, D. F., Babcock, G. T., and Yocum, C. F. (1984) *Biochim. Biophys. Acta 765*, 388−398.
26. de Paula, J. C., Innes, J. B., and Brudvig, G. W. (1985) *Biochemistry 24*, 8114−8120.
27. Briantais, J.-M., Vernotte, C., Miyao, M., Murata, N., and Picaud, M. (1985) *Biochim. Biophys. Acta 808*, 348−351.
28. Ikeuchi, M., and Inoue, Y. (1986) *Arch. Biochem. Biophys. 247*, 97−107.
29. Thompson, L. K., Miller, A.-F., Buser, C. A., de Paula, J. C., and Brudvig, G. W. (1989) *Biochemistry 28*, 8048−8056.
30. van Leeuwen, P. J., Nieveen, M. C., van de Meent, E. J., Dekker, J. P., and van Gorkom, H. J. (1991) *Photosynth. Res. 28*, 149−153.
31. Garbers, A., Kurreck, J., Reifarth, F., Renger, G., and Parak, F. (1996) in *Proceedings of the International Conference on the Applied Mossbauer Effect* (Ortalli, I., Ed.) Vol. 50, pp 811−814, SIF, Bologna, Italy.

32. Renger, G., Kurreck, J., Reifarth, F., Haag, E., Bergmann, A., Parak, F., Garbers, A., McMillan, F., Lendzian, F., and Lubitz, W. (1997) in *Bioinorganic Chemistry* (Trautwein, A., Ed.) pp 260−277, VCH Publishers, Weinheim, Germany.
33. Yamada, Y., Tang, X.-S., Itoh, S., and Satoh, K. (1987) *Biochim. Biophys. Acta 891*, 129−137.
34. Nagatsuka, T., Fukuhara, S., Akabori, K., and Toyoshima, Y. (1991) *Biochim. Biophys. Acta 1057*, 223−231.
35. MacDonald, G. M., Boerner, R. J., Everly, R. M., Cramer, W. A., Debus, R. J., and Barry, B. A. (1994) *Biochemistry 33*, 4393−4400.
36. Shuvalov, V. A., Heber, U., and Schreiber, U. (1989) *FEBS Lett. 258*, 27−31.
37. Dekker, J. P., Bowlby, N. R., and Yocum, C. F. (1989) *FEBS Lett. 254*, 150−154.
38. Gounaris, K., Chapman, D. J., Booth, P., Crystall, B., Giorgi, L. B., Klug, D. R., Porter, G., and Barber, J. (1990) *FEBS Lett. 265*, 88−92.
39. Montoya, G., Yruela, I., and Picorel, R. (1991) *FEBS Lett. 283*, 255−258.
40. Babcock, G. T., Widger, W. R., Cramer, W. A., Oertling, W. A., and Metz, J. G. (1985) *Biochemistry 24*, 3638−3645.
41. Moskalenko, A. A., Barbato, R., and Giacometti, G. M. (1992) *FEBS Lett. 314*, 271−274.
42. McNamara, V. P., Sutterwala, F. S., Pakrasi, H. B., and Whitmarsh, J. (1997) *Proc. Natl. Acad. Sci. U.S.A. 94*, 14173−14178.
43. Francke, C., Loyal, R., Ohad, I., and Haehnel, W. (1999) *FEBS Lett. 442*, 75−78.
44. Vallon, O., Tae, G.-S., Cramer, W. A., Simpson, D., Hoyer-Hansen, G., and Bogorad, L. (1989) *Biochim. Biophys. Acta 975*, 132−141.
45. Tae, G.-S., and Cramer, W. A. (1994) *Biochemistry 33*, 10060−10068.
46. Ortega, J. M., Hervas, M., and Losada, M. (1989) *Z. Naturforsch. 44c*, 415−422.
47. Fan, H. N., and Cramer, W. A. (1970) *Biochim. Biophys. Acta 216*, 200−207.
48. Erixon, K., Losier, R., and Butler, W. L. (1972) *Biochim. Biophys. Acta 267*, 375−382.
49. Horton, P., Witmarsh, J., and Cramer, W. A. (1976) *Arch. Biochem. Biophys. 176*, 519−524.
50. Horton, P., and Croze, E. (1977) *Biochim. Biophys. Acta 462*, 86−101.
51. Rich, P. R., and Bendall, D. S. (1980) *Biochim. Biophys. Acta 591*, 153−161.
52. Ortega, J. M., Hervas, M., and Losada, M. (1992) in *Research in Photosynthesis* (Murata, N., Ed.) Vol. 2, pp 697−700, Kluwer Academic Publishers, Dordrecht, The Netherlands.
53. Ortega, J. M., Hervas, M., and Losada, M. (1988) *Eur. J. Biochem. 171*, 449−455.
54. Iwasaki, I., Tamura, N., and Okayama, S. (1995) *Plant Cell Physiol. 36*, 583−589.
55. McNamara, V. P., and Gounaris, K. (1995) *Biochim. Biophys. Acta 1231*, 289−296.
56. Cox, R. P., and Bendall, D. S. (1972) *Biochim. Biophys. Acta 283*, 124−135.
57. Wada, K., and Arnon, D. I. (1971) *Proc. Natl. Acad. Sci. U.S.A. 68*, 3064−3068.
58. Ortega, J. M., Hervas, M., and Losada, M. (1990) *Plant Sci. 68*, 71−75.
59. Bricker, T. M., Pakrasi, H. B., and Sherman, L. A. (1985) *Arch. Biochem. Biophys. 237*, 170−176.
60. Ghanotakis, D. F., Demetriou, D. M., and Yocum, C. F. (1987) *Biochim. Biophys. Acta 891*, 15−21.
61. Völker, M., Ono, T., Inoue, Y., and Renger, G. (1985) *Biochim. Biophys. Acta 806*, 25−34.
62. Haag, E., Irrgang, K. D., Boekema, E., and Renger, G. (1990) *Eur. J. Biochem. 189*, 47−53.
63. Völker, M., Renger, G., and Rutherford, A. W. (1986) *Biochim. Biophys. Acta 851*, 424−430.
64. Ahmad, I., Giorgi, L. B., Barber, J., Porter, G., and Klug, D. R. (1993) *Biochim. Biophys. Acta 1143*, 239−242.
65. Shuvalov, V. A., Schreiber, U., and Heber, U. (1994) *FEBS Lett. 337*, 226−230.
66. Gadjieva, R., Mamedov, F., Renger, G., and Styring, S. (1998) in *Photosynthesis: Mechanisms and Effects* (Garab, G., Ed.) Vol. II, pp 1101−1104, Kluwer Academic Publishers, Dordrecht, The Netherlands.
67. Gadjieva, R., Mamedov, F., Renger, G., and Styring, S. (1999) *Biochemistry 38*, 10578−10584.
68. Krishtalik, L. I., Tae, G.-S., Cherepanov, W. A., and Cramer, W. A. (1993) *Biophys. J. 65*, 184−195.
69. Hulsebosch, R. J., Kaminskaya, O. P., Hoff, A. J., and Shuvalov, V. A. (1999) (manuscript in preparation).
70. Nanba, O., and Satoh, K. (1987) *Proc. Natl. Acad. Sci. U.S.A. 84*, 109−112.
71. Racker, E., Violand, B., O'Neal, S., Alfonzo, M., and Telford, J. (1979) *Arch. Biochem. Biophys. 198*, 470−477.
72. Berthold, D. A., Babcock, G. T., and Yocum, C. F. (1981) *FEBS Lett. 134*, 231−234.
73. Irrgang, K. D., Lekauskas, A., Franke, P., Reifarth, F., Smolian, H., Karge, M., and Renger, G. (1998) in *Photosynthesis: Mechanisms and Effects* (Garab, G., Ed.) Vol. II, pp 977−980, Kluwer Academic Publishers, Dordrecht, The Netherlands.
74. Cramer, W. A., Theg, S. M., and Widger, W. R. (1986) *Photosynth. Res. 10*, 393−403.
75. Porra, R. J., Thompson, W. A., and Kriedemann, P. E. (1989) *Biochim. Biophys. Acta 975*, 384−394.
76. Renger, G. (1972) *Biochim. Biophys. Acta 256*, 428−439.
77. Weiss, W., and Renger, G. (1986) *Biochim. Biophys. Acta 850*, 173−183.
78. Dutton, P. L. (1971) *Biochim. Biophys. Acta 226*, 63−80.
79. Barber, J., and De Las Rivas, J. (1993) *Proc. Natl. Acad. Sci. U.S.A. 90*, 10942−10946.
80. Ortega, J. M., Hervas, M., de la Rosa, M. A., and Losada, M. (1994) *J. Plant Physiol. 144*, 454−461.
81. Kurreck, J., Garbers, A., Reifarth, F., Andreasson, L.-E., Parak, F., and Renger, G. (1996) *FEBS Lett. 381*, 53−57.
82. Fujita, I., Davies, M. S., and Fajer, J. (1978) *J. Am. Chem. Soc. 100*, 6280−6282.
83. Vacha, F., Josef, D. M., Durant, J. R., Telfer, A., Klug, D. R., Porter, G., and Barber, J. (1995) *Proc. Natl. Acad. Sci. U.S.A. 92*, 2929−2933.
84. Alizadeh, S., Barber, J., and Nixon, P. (1995) in *Photosynthesis: from Light to Biosphere* (Mathis, P., Ed.) Vol. 1, pp 895−898, Kluwer Academic Publishers, Dordrecht, The Netherlands.
85. Murata, N., Higashi, S. I., and Fujimura, Y. (1990) *Biochim. Biophys. Acta 1019*, 261−268.
86. Tezcan, F. A., Winkler, J. R., and Gray, H. R. (1998) *J. Am. Chem. Soc. 120*, 13383−13388.
87. Santini, C., Tidu, V., Tognon, G., Magaldi, A. G., and Bassi, R. (1994) *Eur. J. Biochem. 221*, 307−315.
88. Hankamer, B., Barber, J., and Bockema, E. J. (1997) *Annu. Rev. Plant Physiol. Plant Mol. Biol. 48*, 641−671.
89. Lyon, M. K. (1998) *Biochim. Biophys. Acta 1364*, 403−419.
90. Ortega, J. M., Hervas, M., De la Rosa, M. A., and Losada, M. (1995) *Photosynth. Res. 46*, 185−191.
91. Matsuda, H., and Butler, W. L. (1983) *Biochim. Biophys. Acta 724*, 123−127.
92. Tang, X.-S., and Diner, B. A. (1994) *Biochemistry 33*, 4594−4603.
93. Mizusawa, N., Yamashita, T., and Miyao, M. (1999) *Biochim. Biophys. Acta 1410*, 273−286.
94. Rhee, K.-H., Morris, E. P., Barber, J., and Kühlbrandt, W. (1998) *Nature 396*, 283−286.
95. Rhee, K.-H., Morris, E. P., Zheleva, D., Hankamer, B., Kühlbrandt, W., and Barber, J. (1997) *Nature 389*, 522−526.

96. Hankamer, B., Morris, E. P., and Barber, J. (1999) *Nat. Struct. Biol. 6*, 560−564.
97. Bergström, J., and Vänngard, T. (1982) *Biochim. Biophys. Acta 682*, 452−456.
98. Malkin, R., and Vänngard, T. (1980) *FEBS Lett. 111*, 228−231.
99. Nugent, J. H. A., and Evans, M. C. W. (1980) *FEBS Lett. 112*, 1−4.
100. de Paula, J. C., Li, P. M., Miller, A.-F., Wu, B. W., and Brudvig, G. W. (1986) *Biochemistry 25*, 6487−6494.
101. Cramer, W. A., Horton, P., and Wever, R. (1975) in *Electron-transfer chains and oxidative phosphorylation* (Quagliariello, E., et al., Eds.) pp 31−36, North-Holland Publishing, Amsterdam, The Netherlands.
102. Renger, G. (1987) *Photosynthetica 21*, 203−224.
103. Berthomieu, C., Boussac, A., Mäntele, W., Breton, J., and Nabedryk, E. (1992) *Biochemistry 31*, 11460−11471.

BI991257G